FV Upwind Stabilization of FE Discretizations for Advection–Diffusion Problems

Fabian Brunner, Florian Frank and Peter Knabner

Abstract We apply a novel upwind stabilization of a mixed hybrid finite element method of lowest order to advection–diffusion problems with dominant advection and compare it with a finite element scheme stabilized by finite volume upwinding. Both schemes are locally mass conservative and employ an upwind-weighting formula in the discretization of the advective term. Numerical experiments indicate that the upwind-mixed method is competitive with the finite volume method. It prevents the appearance of spurious oscillations and produces nonnegative solutions for strongly advection-dominated problems, while the amount of artificial diffusion is lower than that of the finite volume method. This makes the method attractive for applications in which too much numerical diffusion is critical and may lead to false predictions; e.g., if highly nonlinear reactive processes take place only in thin interaction regions.

1 Introduction

In this article, we consider the linear advection–diffusion equation

$$\partial_t u - \nabla \cdot (D \nabla u - \mathbf{Q} u) = 0 \quad \text{in } J \times \Omega \tag{1}$$

(and semilinear system variants thereof) on a finite time interval $J =]0, t_{\text{end}}]$ and a polygonally bounded convex domain $\Omega \subset \mathbb{R}^2$. Equation (1) serves as a model for

F. Brunner (✉) · F. Frank · P. Knabner
Department of Mathematics, University of Erlangen–Nuremberg, Cauerstr. 11,
91058 Erlangen, Germany
e-mail: brunner@math.fau.de

F. Frank
e-mail: frank@math.fau.de

P. Knabner
e-mail: knabner@math.fau.de

many natural processes, e.g., heat transfer or mass transport in porous media. The physical principle underlying this equation is conservation of mass, which should be reflected by any numerical method that is used for discretization.

The numerical simulation of (1) becomes particularly challenging if the advective term dominates the diffusive term, i.e., when the Péclet number is large. Then, sharp fronts in the solution cannot be resolved properly by conventional numerical schemes, which typically produce solutions that are polluted by spurious oscillations. To circumvent this, various approaches with different strengths and weaknesses were proposed in the literature. One of the most widely used techniques to handle advection dominance is upwinding, which is easy to implement and which preserves monotonicity well at the cost of introducing additional diffusion to the problem. It relies on the simple idea of discretizing the advection term as a function of the flow direction.

In this work, we compare a novel upwind stabilization of a mixed hybrid finite element scheme, which was studied numerically in [8] and analytically in [4] with a linear finite element scheme that uses an upwind finite volume approximation of the advective term. The latter was used in [5] to incorporate upwinding into an existing linear finite element code and thus to recover the discrete maximum principle, which is violated if linear finite elements are applied to advection-dominated transport problems.

By means of two test scenarios, we demonstrate that the upwind-mixed hybrid method is competitive with the finite volume upwind method with respect to robustness, monotonicity properties, and the amount of artificial numerical diffusion introduced by the schemes.

The rest of the work is organized as follows. In Sect. 2, the basic notation and the most important functional spaces are introduced. In Sect. 3, the discretization of problem {(1), (2)} with the two schemes under consideration is briefly sketched. Finally, Sect. 4 contains the description and the results of the test scenarios.

2 Notation and Problem Statement

Let the boundary $\partial\Omega$ decompose into a Dirichlet part $\partial\Omega_D$, a Neumann part $\partial\Omega_N$, and a flux part $\partial\Omega_{flux}$ with outward unit normal $\mathbf{n}$. In order to obtain a well-posed problem, Eq. (1) is supplemented by the following initial and boundary conditions:

$$u = u_D \qquad\qquad \text{on } J \times \partial\Omega_D, \qquad (2a)$$

$$-D\nabla u \cdot \mathbf{n} = 0 \qquad\qquad \text{on } J \times \partial\Omega_N, \qquad (2b)$$

$$-D\nabla u \cdot \mathbf{n} + u\,\mathbf{Q} \cdot \mathbf{n} = 0 \qquad\qquad \text{on } J \times \partial\Omega_{flux}, \qquad (2c)$$

$$u = u^0 \qquad\qquad \text{on } \{0\} \times \Omega \qquad (2d)$$

with u_D and u_0 given. All coefficients are assumed to be sufficiently smooth.

Let the time interval J be decomposed into N subintervals of equal length and let $\Delta t := t_{end}/N$ denote the time step size. Let $\mathcal{T}_h$ be a regular family of decomposi-

tions into closed triangles T of characteristic size h such that $\overline{\Omega} = \cup T$. We denote by $\mathbb{P}_k(T)$ the space of polynomials of degree at most k on a triangle $T \in \mathscr{T}_h$ and define by $\mathbb{RT}_0(T) := \{\mathbf{v} : T \to \mathbb{R}^2 \mid \mathbf{v}(\mathbf{x}) = a\mathbf{x} + \mathbf{b}, \ a \in \mathbb{R}, \ \mathbf{b} \in \mathbb{R}^2\}$ the local Raviart–Thomas space. Moreover, let $\mathbb{P}_k(\mathscr{T}_h) := \{w_h : \overline{\Omega} \to \mathbb{R} \mid \forall T \in \mathscr{T}_h, w_h|_T \in \mathbb{P}_k(T)\}$ denote the (discontinuous) global polynomial space on the triangulation $\mathscr{T}_h$ and let $\mathbb{P}_1^c(\mathscr{T}_h) := C(\overline{\Omega}) \cap \mathbb{P}_1(\mathscr{T}_h)$. The set of edges of $\mathscr{T}_h$ is denoted by $\mathscr{E}$ and that of $T \in \mathscr{T}_h$ by $\mathscr{E}(T)$, where we omit the index $_h$ here. Finally, let the space $H^1(\Omega)$ contain those functions of $L^2(\Omega)$ which have a weak derivative in $L^2(\Omega)$, and let $H_{0,\mathrm{D}}^1(\Omega)$ denote the subspace of $H^1(\Omega)$ consisting of functions with vanishing trace on $\partial\Omega_\mathrm{D}$.

3 Numerical Schemes

The two numerical schemes under consideration are outlined in the following. The first one is a linear finite element scheme that uses an upwind finite volume approximation of the advective term (LFEMstab) as presented in [5]. The second one is a mixed hybrid finite element scheme combined with an upwind-weighting formula based on the Lagrange multipliers (MHFEMstab), which are introduced into the formulation by hybridization; cf. [2, 4]. For ease of presentation, we assume that $u_\mathrm{D} = 0$ and we use full upwinding in the sequel. However, the schemes can be easily extended to inhomogeneous Dirichlet data and to more sophisticated upwind formulas, e.g., partial upwinding [6].

3.1 Scheme: LFEMstab

The discretization of $\{(1), (2)\}$ with piecewise linear, globally continuous finite elements in space and with the implicit Euler method in time yields the following discrete problem.
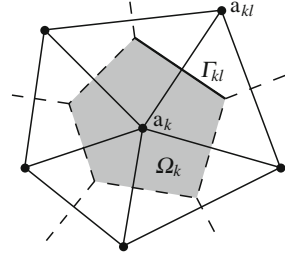
Let $n \in \{1, \ldots, N\}$ and let $u_h^{n-1} \in \mathbb{P}_1^c(\mathscr{T}_h) \cap H_{0,\mathrm{D}}^1(\Omega)$ be given. Find $u_h^n \in \mathbb{P}_1^c(\mathscr{T}_h) \cap H_{0,\mathrm{D}}^1(\Omega)$ such that

$$\frac{1}{\Delta t} \int_\Omega (u_h^n - u_h^{n-1}) z_h + \int_\Omega D\nabla u_h^n \cdot \nabla z_h + \int_\Omega z_h \nabla \cdot (\mathbf{Q} u_h^n) = 0$$

for all $z_h \in \mathbb{P}_1^c(\mathscr{T}_h) \cap H_{0,\mathrm{D}}^1(\Omega)$.

Let φ_k be the basis function of $\mathbb{P}_1^c(\mathscr{T}_h)$ that is associated with node $\mathbf{a}_k$, i.e., $\varphi_k(\mathbf{a}_j) = \delta_{kj}$ holds. Since φ_k has a local support on the triangles around $\mathbf{a}_k$, the advection term can be approximated by

Fig. 1 Control volume Ω_k associated with the node $\mathbf{a}_k$ according to the Voronoi diagram of $\mathscr{T}_h$. The support of $\varphi_k \in \mathbb{P}_1^c(\mathscr{T}_h)$ is the union of all triangles containing the vertex $\mathbf{a}_k$

$$\int_{\Omega} \varphi_k \nabla \cdot (\mathbf{Q} u_h^n) \approx \int_{\Omega_k} \nabla \cdot (\mathbf{Q} u_h^n) = \int_{\partial \Omega_k} u_h^n \, \mathbf{Q} \cdot \mathbf{n} = \sum_j \int_{\Gamma_{kj}} u_h^n \, \mathbf{Q} \cdot \mathbf{n} \,,$$

where Ω_k is the Voronoi cell around $\mathbf{a}_k$, the boundary of which decomposes into line segments Γ_{kl}, $l \in \{1, 2, \ldots\}$, cf. Fig. 1. The boundary integral on Γ_{kl} can now be treated with a finite volume upwind scheme:

$$\int_{\Gamma_{kl}} u_h^n \, \mathbf{Q} \cdot \mathbf{n} \approx |\Gamma_{kl}| \, \alpha_{kl}(u_h^n) \, \mathbf{Q} \left(\frac{\mathbf{a}_k + \mathbf{a}_{kl}}{2} \right) \cdot \mathbf{n}$$

with $\mathbf{n}$ still denoting the unit normal pointing outward of Ω_k and with $\mathbf{a}_{kl}$ denoting the reflection of node $\mathbf{a}_k$ across Γ_{kl}. The function α for a full upwind scheme reads

$$\alpha_{kl}(u_h^n) := \begin{cases} u_h^n(\mathbf{a}_k) & \text{if } \mathbf{Q} \cdot \mathbf{n} \geq 0 \text{ at } (\mathbf{a}_k + \mathbf{a}_{kl})/2 \quad (\text{outflow of } \Omega_k) \,, \\ u_h^n(\mathbf{a}_{kl}) & \text{otherwise} \quad (\text{inflow into } \Omega_k) \,. \end{cases}$$

Using Voronoi cells as control volumes, for nonobtuse triangular meshes, LFEM-stab is equivalent to the classical cell centered finite volume method if diffusion is cellwise constant, cf. [6]. Therefore, LFEMstab is locally mass conservative and provides formally first order accurate approximations of the scalar unknown u in $L^2(\Omega)$.

3.2 Scheme: MHFEMstab

In this section, the discretization of $\{(1), (2)\}$ using the upwind-stabilized mixed hybrid finite element scheme of [4] is sketched. It relies on an Euler-implicit time stepping scheme and lowest order Raviart–Thomas finite elements for the spatial discretization. In contrast to non-hybrid schemes, the continuity constraints on the normal fluxes are not incorporated into the function space, but are ensured by introducing additional variables—the Lagrange multipliers—along with additional equations. More precisely, the space

$$\mathbf{V}_h := \{\mathbf{v} \in (L^2(\Omega))^2 \mid \forall T \in \mathscr{T}_h, \ \mathbf{v}|_T \in \mathbb{RT}_0(T)\}$$

is used as the ansatz space for the discrete approximation of the mass flux $\mathbf{q} := -D\nabla u + \mathbf{Q}u$. The Lagrange multipliers are taken from the space

$$\Lambda_h := \{\lambda \in L^2(\mathscr{E}) \mid \forall E \in \mathscr{E}, \ \lambda|_E \in \mathbb{P}_0(E); \ \forall E \in \mathscr{E}_D, \ \lambda|_E = 0\},$$

where $\mathscr{E}$ denotes the set of interior edges and $\mathscr{E}_D$ the set of Dirichlet edges. Finally, the scalar unknown is approximated in the space $W_h := \mathbb{P}_0(\mathscr{T}_h)$.

The definition of the upwind-mixed hybrid scheme involves the discrete velocity field $\mathbf{Q}_h^n := \Pi_h \mathbf{Q}^n$, where Π_h denotes the usual Raviart–Thomas projection operator. We assume that $\mathbf{Q}_h^n$ has the representation $\mathbf{Q}_h^n = \sum_{T \in \mathscr{T}_h} \sum_{E \in \mathscr{E}(T)} Q_{TE}^n \mathbf{v}_{TE}$ in a basis $\{\mathbf{v}_{TE}\}_{T \in \mathscr{T}_h, E \in \mathscr{E}(T)}$ of $\mathbf{V}_h$. Basis functions of W_h and Λ_h are given by characteristic functions $\{\chi_T\}_{T \in \mathscr{T}_h}$ and $\{\mu_E\}_{E \in \mathscr{E}}$, respectively. The scheme MHFEMstab reads as follows.

Let $n \in \{1, \ldots, N\}$ and let $u_h^{n-1} \in W_h$ be given. Find $(\mathbf{q}_h^n, u_h^n, \lambda_h^n) \in \mathbf{V}_h \times W_h \times \Lambda_h$ with $\mathbf{q}_h^n = \sum_{T \in \mathscr{T}_h} \sum_{E \in \mathscr{E}(T)} q_{TE}^n \mathbf{v}_{TE}, u_h^n = \sum_{T \in \mathscr{T}_h} u_T^n \chi_T, \lambda_h^n = \sum_{E \in \mathscr{E}_\Omega} \lambda_E^n \mu_E$ such that

$$\int_\Omega D^{-1} \mathbf{v}_h \cdot \mathbf{q}_h^n - \int_\Omega u_h^n \nabla \cdot \mathbf{v}_h$$

$$- \sum_{T \in \mathscr{T}_h} \sum_{E \in \mathscr{E}(T)} Q_{TE}^n \alpha_{TE}(u_T^n, \lambda_E^n) \int_T D^{-1} \mathbf{v}_h \cdot \mathbf{v}_{TE} = - \sum_{T \in \mathscr{T}_h} \int_{\partial T} \lambda_h^n \mathbf{v}_h \cdot \mathbf{n}, \quad \text{(3a)}$$

$$\frac{1}{\Delta t} \int_\Omega (u_h^n - u_h^{n-1}) w_h + \int_\Omega w_h \nabla \cdot \mathbf{q}_h^n = 0, \quad \text{(3b)}$$

$$\sum_{T \in \mathscr{T}_h} \int_{\partial T} \mu_h \mathbf{q}_h^n \cdot \mathbf{n} = 0 \quad \text{(3c)}$$

for all $(\mathbf{v}_h, w_h, \mu_h) \in \mathbf{V}_h \times W_h \times \Lambda_h$, where the upwind weights are defined as

$$\alpha_{TE}(u_T^n, \lambda_E^n) = \begin{cases} u_T^n & \text{if } Q_{TE}^n \geq 0, \\ \lambda_E^n & \text{otherwise}. \end{cases} \quad \text{(4)}$$

The function α_{TE} takes the flow direction into account: If $Q_{TE}^n \geq 0$, i.e., if there is an outflow across the edge E, the value u_T^n on the current triangle is used to discretize the advective term. Otherwise, the Lagrange multiplier λ_E^n—which represents an approximation of u^n on E—is used. Note that the definition (4) of α_{TE} is slightly different than that in [4, 8], where $\alpha_{TE}(u_T^n, \lambda_E^n) := 2\lambda_E^n - u_T^n$ was used if $Q_{TE}^n < 0$. This is because less numerical diffusion was observed using (4). The proof of convergence in [4], however, applies to either choice.

Since the basis functions of $\mathbf{V}_h$ can be chosen to have support only on a single mesh element, static condensation is usually employed in standard cell-centered mixed hybrid schemes in order to reduce the number of global unknowns by local elimination. With the specific choice of α_{TE} in the above scheme, Eq. (3a) remains fully local and static condensation may be applied further on. Therefore, the upwind-mixed hybrid scheme can be implemented more efficiently than standard upwind-mixed schemes that use information from neighbor elements to discretize the advection term, cf. [4].

4 Robustness of the Schemes

In the following, the schemes LFEMstab and MHFEMstab presented in Sect. 3 and their non-stabilized versions LFEM and MHFEM are compared with respect to numerical attributes that are essential for reliable simulation of advection-dominated flows, e.g., monotonicity and the amount of artificial diffusion they introduce.

4.1 Scenario: Pulse

We consider a time interval $J :=]0, 1]$ using a time step size of $\Delta t := 5\text{E}{-}3$ and a rectangular domain $\Omega :=]0, 2[\times]0, 1[$ with $\partial \Omega_N = \{2\} \times [0, 1]$ and $\partial \Omega_{\text{flux}} = \partial \Omega \setminus \partial \Omega_N$, which is triangulated by an unstructured grid containing 2, 704 triangles. We choose the following data in $\{(1), (2)\}$: $D := 2\text{E}{-}4$, $\mathbf{Q} := (1, 0)^T$, and $u^0 := 1$ on $[1/4, 3/4]^2$ and zero elsewhere.

The center of mass of the initial (quadratic) distribution u^0 should be transported to $\mathbf{x} = (1.5, 0.5)^T$ by advection and be slightly smeared by diffusion. Figure 2 shows the distribution of u_h at t_{end} for the four schemes under investigation. The non-stabilized schemes LFEM and MHFEM produce oscillations that reach negative values. Although the MHFEM solution at t_{end} is closer to the expected one, the oscillations are stronger and lead to non-convergence shortly after t_{end}, which is not the case with LFEM. Both of the stabilized schemes LFEMstab and MHFEMstab conserve the nonnegativity of u^0, however, MHFEMstab adds less artificial diffusion to the solution.

4.2 Scenario: Contaminant Biodegradation

As a second example, we consider the simulation of contaminant biodegradation according to a simplified Monod model. This nonlinear test problem was used by several authors, cf. [1, 3, 7], to compare different numerical schemes with respect to the numerical diffusion they introduce. It illustrates that prognoses of methods with
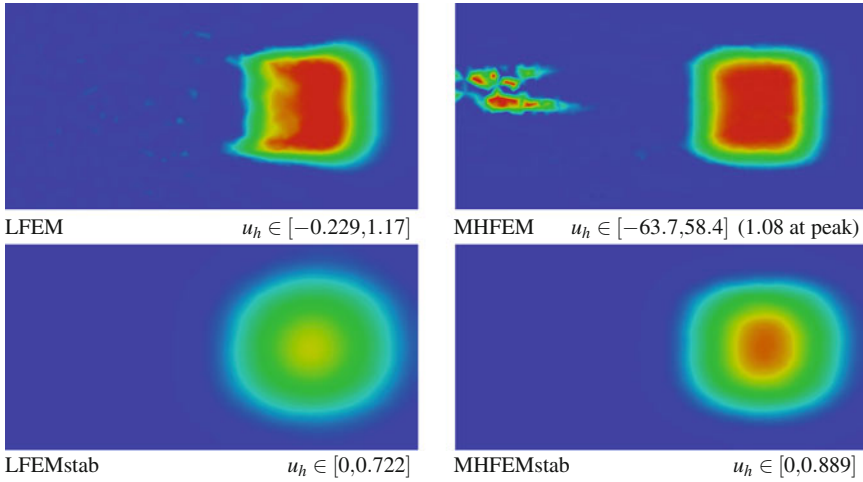
| LFEM | $u_h \in [-0.229, 1.17]$ | MHFEM | $u_h \in [-63.7, 58.4]$ (1.08 at peak) |
| LFEMstab | $u_h \in [0, 0.722]$ | MHFEMstab | $u_h \in [0, 0.889]$ |

Fig. 2 The distribution of u_h at t_{end} for the different schemes under investigation. The color scaling is fixed from zero *(blue)* to one *(red)*; the global minima and maxima are listed below each plot

large artificial diffusion can be completely wrong. Precisely, a degradation reaction between an electron donor u_{don} (e.g. a contaminant) and an electron acceptor u_{acc} (e.g. oxygen) is considered, which is catalyzed by a bio species u_{bio}. As a simplification, biomass growth is neglected and the process is modeled by the equations

$$\partial_t(\theta u_i) - \nabla \cdot (\theta D \nabla u_i - \mathbf{Q} u_i) = \alpha_i \mu , \quad i \in \{\text{don, acc}\}$$

with the Monod reaction rate $\mu = -u_{bio} u_{don}(K_{don} + u_{don})^{-1} u_{acc}(K_{acc} + u_{acc})^{-1}$. For the simulation the following data are used: $\Omega =]0, 0.5[\times]0, 1[$, $\theta = 0.2$, $D = 10\text{E}{-}4$, $\mathbf{Q} = (0, -1)^T$, $\alpha_{don} = 5$, $\alpha_{acc} = 0.5$, $K_{don} = 0.1$, $K_{acc} = 0.1$, $u_{bio} = 1$. As initial conditions, $u_{don}^0 = 0$ and $u_{acc}^0 = 0.1$ are chosen in Ω. The electron donor is injected at the middle part of the upper boundary and transported toward the lower boundary by advection. The stationary Dirichlet boundary conditions are given by $u_{don} = 1$ and $u_{acc} = 0$ on $]0.225, 0.275[\times \{1\}$ and $u_{don} = 0$ and $u_{acc} = 0.1$ elsewhere on the upper boundary, respectively. The degradation reaction takes place only in those parts of the domain where the concentrations of both species are sufficiently large, which is the case at the interface between the electron donor and the surrounding area, where still enough electron acceptor is available. Thus, numerical methods introducing much artificial diffusion lead to an overestimation of the mixing zone of the two species, and the contaminant is degraded too fast in this case.

Figure 3 shows the predicted contaminant concentrations using LFEMstab and MHFEMstab on a locally preadapted unstructured grid with 1, 988 elements at t_{end}, where a steady state has been reached. For both schemes, Newton's method was used for the linearization of the nonlinear reaction terms. We observe that both methods
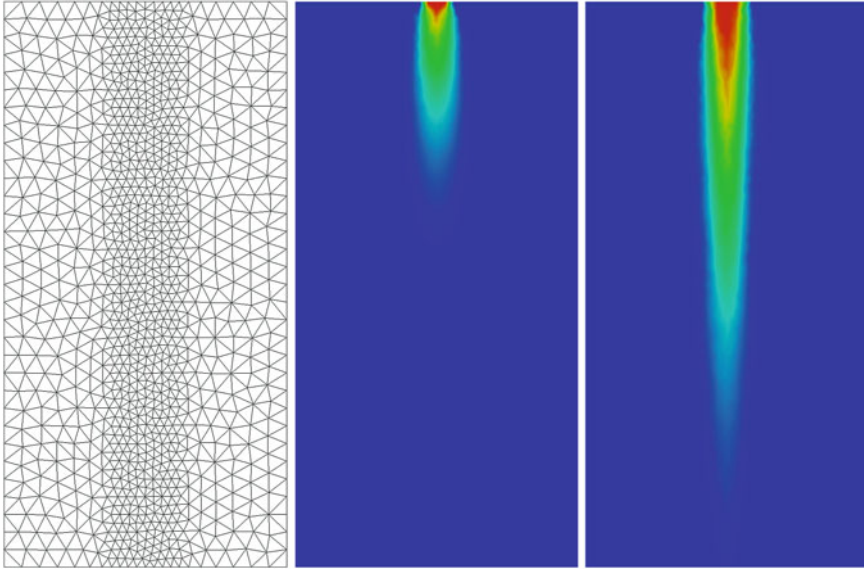
Fig. 3 Locally preadapted grid *(left)* and computed concentration profiles for $u_{\text{don},h}$ using LFEM-stab *(center)* and MHFEMstab *(right)*. The values of $u_{\text{don},h}$ are in [0, 1] for both methods

produce nonnegative solutions. On this relatively coarse grid, LFEMstab predicts a complete degradation of the contaminant within the computational domain, which is incorrect and may have serious consequences in practice. The contaminant plume computed by MHFEMstab, however, covers the full length of the domain and reaches the outflow boundary. This is in accordance with a reference solution we computed on a grid with 250,000 elements.

5 Conclusion

We conclude that the upwind-mixed hybrid method provides a suitable scheme for simulating advection-driven transport problems. Compared to the finite volume method the amount of artificial diffusion appears to be lower, which is important in applications where the dominating processes take place in small interaction regions. Moreover, similarly to the classical cell-centered mixed method, it is fully hybridizable, and the incorporation of upwinding does not increase the computational costs in contrast to standard upwind-mixed methods.

References

1. Bause, M., Knabner, P.: Numerical simulation of contaminant biodegradation by higher order methods and adaptive time stepping. Comput. Vis. Sci. **7**, 61–78 (2004)
2. Boffi, D., Brezzi, F., Fortin, M.: Mixed Finite Element Methods and Applications. Springer, Berlin (2013)
3. Brunner, F., Radu, F.A., Bause, M., Knabner, P.: Optimal order convergence of a modified BDM_1 mixed finite element scheme for reactive transport in porous media. Adv. Water Resour. **35**, 163–171 (2012)
4. Brunner, F., Radu, F.A., Knabner, P.: Analysis of an upwind-mixed hybrid finite element method for transport problems. SIAM J. Num. Anal. **52**(1), 83–102 (2014)
5. Hoffmann, J.: Reactive transport and mineral dissolution/precipitation in porous media: efficient solution algorithms, benchmark computations and existence of global solutions. Ph.D. thesis, Friedrich–Alexander University of Erlangen–Nuremberg (2010)
6. Knabner, P., Angermann, L.: Numerical Methods for Elliptic and Parabolic Partial Differential Equations. Springer, New York (2003)
7. Ohlberger, M., Rohde, C.: Adaptive finite volume approximations of weakly coupled convection dominated parabolic systems. IMA J. Numer. Anal. **22**, 253–280 (2002)
8. Radu, F.A., Suciu, N., Hoffmann, J., Vogel, A., Kolditz, O., Park, C.H., Attinger, S.: Accuracy of numerical simulations of contaminant transport in heterogeneous aquifers: a comparative study. Adv. Water Resour. **34**(1), 47–61 (2011)